Spatial Structures of Dipolar Ferromagnetic Liquids

B. Groh and S. Dietrich

Fachbereich Physik, Bergische Universität Wuppertal, D-42097 Wuppertal, Federal Republic of Germany

(Received 20 March 1997)

We have determined the magnetization structure in a ferromagnetic dipolar fluid by performing a numerical minimization of a free energy density functional which is highly nonlocal due to the long range of the dipolar interactions. In a cubic sample a vortex structure is found which consists of four domains and four thick domain walls. Depending on sample size and temperature, near the vortex line we observe an "escape" of the planar magnetization into the normal direction or a reduction of its magnitude inside the vortex core. We describe the temperature dependence of the structure upon approaching the Curie point. If an external field is applied, a transition to a homogeneously magnetized state takes place at a critical field strength. [S0031-9007(97)03661-2]

PACS numbers: 75.50.Mm, 61.30.Cz, 75.70.Kw

The occurrence of a ferromagnetic *liquid* phase without long-ranged positional order has been claimed for strongly dipolar fluids at high densities [1–11] and for supercooled liquid CoPd alloys [12,13]. In this Letter we focus on the former case but the results may also be relevant for the latter case. Evidence for long-ranged orientational order in simple model fluids consisting of spherical particles with permanent dipole moments has been obtained in Monte Carlo simulations [1–6] and in different theoretical approaches [7–11]. These models could also apply to ferrofluids, i.e., colloidal suspensions of solid ferromagnetic particles. Experimentally ferrofluids exhibit strongly paramagnetic behavior but a transition to a ferromagnetic phase might be attainable at high concentrations by appropriate chemical tailoring. Both in simulations and in analytic theories the dipolar forces must be treated carefully due to their long range which may give rise to effects depending on the shape of the sample. It turns out that for all sample shapes, with the exception of a long needle, the equilibrium configuration is inhomogeneous with a spatially varying magnetization $\mathbf{M}(\mathbf{r})$ [14,15]. This implies a shape *independent* free energy, as is expected on general grounds [16]. (These effects are absent in Heisenberg fluids [17] in which the magnetic exchange interaction is short ranged.) The difficult problem of determining explicitly the spatial distribution of the inhomogeneous magnetization for a given sample shape has not yet been solved. Recently we obtained [15] a general characterization of the equilibrium configurations, which, however, does not determine the actual structure. We also speculated about possible domain structures in a cubic sample under the constraint of a discontinuous change of the orientational order across sharp domain boundaries and constant magnetization within the domains. This assumption is obviously unrealistic for liquid systems. Furthermore it implies the existence of line singularities where three or four domains meet each other. However, due to general topological arguments [18], stable line singularities cannot exist in three-dimensional spin systems. Therefore, the actual domain structure within a liquid ferromagnet remains an open problem. In the present work we have succeeded in determining this structure for a cubic sample by using a versatile numerical minimization of an approximate microscopic density functional [10,11,15] for the ferromagnetically ordered fluid. Our approach, which is capable of describing the structure both on the scale of the system size and on a microscopic scale determined by the particle diameter, allows us to analyze simultaneously large scale structures and, for example, the cores of topological defects. Our results feature, *inter alia*, the dissolution of line defects in favor of point defects, the absence of sharp domain walls, the escape of the orientational order into the third dimension, and the loss of order within the cores of the defects.

We have made no *a priori* assumptions regarding the symmetry of the domain structure and have minimized with respect to the dimensionless local magnetization $\mathbf{M}(\mathbf{R})$ at mesh points $\mathbf{R}$ on a simple cubic lattice within the sample. (The actual magnetization is $\sqrt{4\pi/3}\,\rho m\mathbf{M}$, where ρ is the number density and m the dipole moment of the particles.) The fluid particles interact according to the Stockmayer pair potential, given by the sum of the dipolar interaction and the isotropic Lennard-Jones potential characterized by an energy scale ϵ and a particle diameter σ. Within the applied approximation scheme [11,15] the free energy difference between the ferromagnetic and the paramagnetic liquid of density ρ is $F = F_{\mathrm{or}} + F_{\mathrm{int}}$. The first contribution, describing the entropy loss due to orientational ordering, is

$$F_{\mathrm{or}} = k_B T\rho \int_V d^3r \int d\cos\theta \,[\tfrac{1}{2} + M(\mathbf{r})\sqrt{12\pi}\cos\theta] \times \ln[1 + M(\mathbf{r})\sqrt{12\pi}\cos\theta] \simeq k_B T\rho a^3 \sum_{\mathbf{R}} \sum_{n=1}^{\infty} \frac{[\sqrt{12\pi}\,M(\mathbf{R})]^{2n}}{(2n-1)2n(2n+1)}\,.$$

It is obtained by an integration over the orientational distribution of the fluctuating dipole moments. Here $M(\mathbf{r})$

is the magnitude of the local magnetization, θ is the angle between the fluctuating and the mean magnetization, and a is the lattice constant of the mesh. The interaction contribution to the free energy is

$$\Delta F_{\rm int} = \tfrac{1}{2} k_B T \rho^2 a^6 \times \sum_{\mathbf{R}} \sum_{\mathbf{R}'} \sum_{i,j} M_i(\mathbf{R}) w_{ij}(\mathbf{R} - \mathbf{R}') M_j(\mathbf{R}'),$$

with the tensor

$$w_{ij}(\mathbf{R}) = \Theta(R - \sigma)[f_{110}(R)\delta_{ij} + f_{112}(R)(\delta_{ij} - 3\hat{R}_i\hat{R}_j)],$$

where $R = |\mathbf{R}|$, $\hat{\mathbf{R}} = \mathbf{R}/R$, and the Heaviside function Θ truncates the interaction at the particle diameter σ. General expressions for the functions f_{110} and f_{112} have been derived in Ref. [19]. For small dipole moments m, $f_{112}(R)$ is proportional to R^{-3} and f_{110} is negligible so that w_{ij} reproduces the well-known form of the dipole-dipole interaction. In an external magnetic field $\mathbf{H}$ a term $-\sqrt{4\pi/3}\,\rho m a^3 \mathbf{H} \cdot \sum_{\mathbf{R}} \mathbf{M}(\mathbf{R})$ must be added to the free energy.

The latter is minimized with respect to the magnetization configuration $\{\mathbf{M}(\mathbf{R})\}$ using simulated annealing [20]. Starting from an appropriate initial configuration, at each step a lattice site $\mathbf{R}_0$ and a new value of $\mathbf{M}(\mathbf{R}_0)$ are chosen at random and the resulting change in free energy ΔF is calculated. The proposed change is accepted with probability $\min\{1, \exp[-\Delta F/(k_B T_s)]\}$, where T_s denotes a control temperature that is gradually reduced during the minimization. Starting from completely random initial states requires extremely long numerical runs. Therefore, in most cases we started from a minimum configuration which had been obtained in a previous run for different parameter values. We used up to $N^3 = 22^3$ mesh points and examined cubic volumes of size $L/\sigma = 4.8$–12.0. Typical CPU times on a workstation were 3.2 hours for a 16^3 mesh and 25 hours for a 22^3 mesh.

As our standard values of the thermodynamic parameters we chose the dipole moment $m^* = \sqrt{m^2/(\sigma^3 \epsilon)} = 1.5$, the temperature $T^* = k_B T/\epsilon = 2.25$, and the density $\rho^* = \rho\sigma^3 = 0.94$. This corresponds to a state well within the ferromagnetic liquid phase as predicted by the present density-functional theory [15]. Figure 1 displays a typical example of the resulting magnetization structures. The section perpendicular to the z axis shows a vortex of closed magnetization lines circulating around this spontaneously chosen axis. In this context it is interesting to note that clusters of some ten to 100 dipolar particles also exhibit a vortex structure at low temperatures [21,22]. The configuration in Fig. 1 may also be described as composed of four domains separated by broad domain walls along the diagonals. Thus it resembles the triangular structure obtained previously [15] under the constraint of sharp domain boundaries. A similar structure has also been found to be the most favorable one in cubic magnetite particles just above the critical single-domain size. However, more complicated structures occur in this case for larger particles [23,24]. As can be seen in the sec-

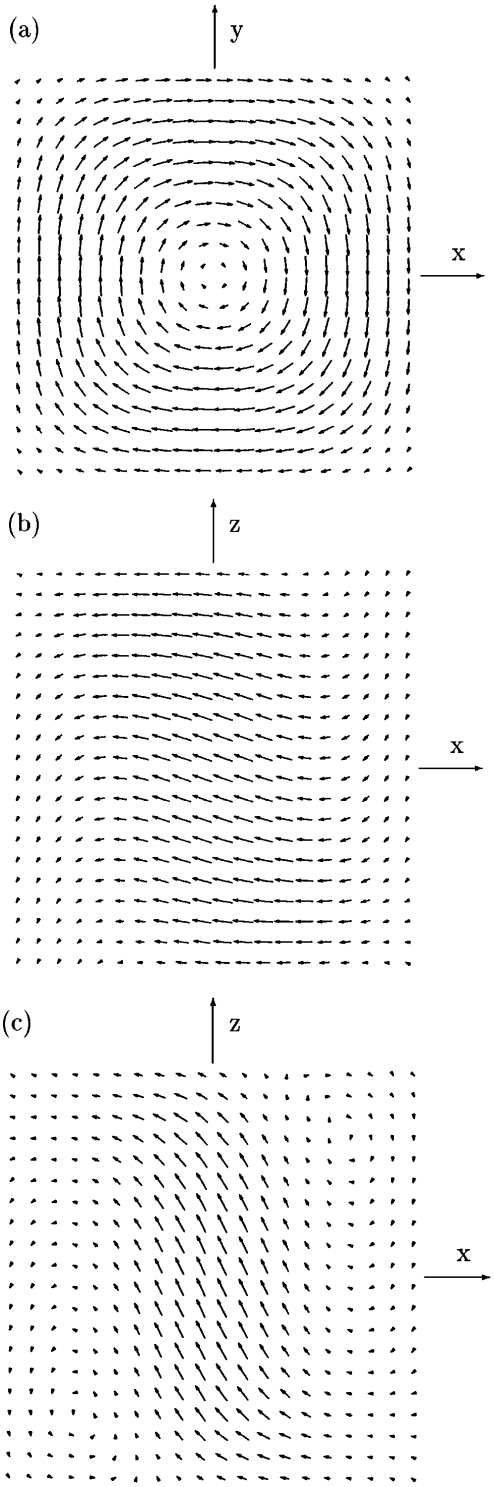

FIG. 1. Magnetization structure of a ferromagnetic liquid in a cubic volume with edge length $L/\sigma = 7.2$, 20^3 mesh points, and $T^* = 2.25$. The three parts of the figure represent sections (a) for fixed $z = 0.025L$, (b) fixed $y = -0.075L$, and (c) fixed $y = -0.225L$; the origin is at the center of the cube. The arrows represent projections of the local magnetization at their midpoint onto the section plane.

tions perpendicular to the y axis, there is a nonvanishing out-of-plane component of $\mathbf{M}(\mathbf{r})$, which is especially pronounced near the vortex axis. In this way a line singularity is avoided by an "escape into the third dimension." This is in accordance with general considerations showing that line singularities are topologically unstable in a system of three-component spins in three spatial dimensions [18], which means that they can always be removed by continuous *local* modifications. However, near the top and the bottom faces of the cube the z component decreases in order to avoid a large normal component at the surface which would produce an unfavorable demagnetization field [15]. Thus, two topologically stable point singularities near the centers of the bottom and top surfaces are inevitable. In contrast to the usual micromagnetic calculations for solids [25], the magnitude of the magnetization is not *a priori* assumed to be a constant, but is included as a minimization parameter. A closer look at the point defects reveals that $|\mathbf{M}(\mathbf{r})|$ strongly decreases inside their cores (see Fig. 2). In the bulk $M(\mathbf{r})$ is approximately constant, but it also decreases near the surfaces.

Very similar structures have been found for all values of L and N. With the exception of the smallest systems the scaling property $\mathbf{M}(\mathbf{r}/\sigma, L/\sigma) = \mathbf{M}^{(0)}(\mathbf{r}/L)$ is approximately obeyed, so that one can surmise that this holds also in the thermodynamic limit. The function $\mathbf{M}^{(0)}$ represents the global texture in the thermodynamic limit.

The domain walls are mainly of the Néel type, i.e., the magnetization rotates within the plane defined by the magnetization directions of the adjacent domains [26]. In order to measure the wall thickness δ we consider the change of the in-plane magnetization component parallel to the wall upon traversing the wall on a normal path. It approaches opposite limits in the adjacent domains. We define δ as the distance between those points where the tangent to this curve at its inflection point reaches these limits [26]. The normalized thickness δ/L decreases slightly from ~ 0.3 to ~ 0.25 within the accessible range of system sizes, but the observed size dependence is compatible with a finite value of δ/L in the thermodynamic limit, which would be in accordance with the scaling behavior proposed above. A finite and nonzero limit of δ/L has already been conjectured by de Gennes and Pincus [27] for liquid ferromagnets and is also expected for an isotropic Heisenberg model, whereas in real solid ferromagnets the wall thickness is always restricted to a microscopic value due to a violation of the full O(N) symmetry induced by the coupling to the lattice anisotropy. In this respect liquid and solid ferromagnets differ significantly.

When the temperature of the fluid is increased the ferromagnetic order vanishes continuously at the Curie temperature T_c. For the small volumes under consideration T_c depends on the system size [28]. It is lowered by about 10% when L/σ is reduced from 9.6 to 4.8. Upon approaching T_c a second mode of avoiding a singularity at the vortex axis evolves: as shown in Fig. 3 a column of less ordered fluid with reduced $M(\mathbf{r})$ develops around this axis, while the degree of escape into the axis direction is reduced. Simultaneously the less ordered surface layer thickens as a consequence of the increasing correlation length near the phase transition.

The above results refer to zero external field. If an external field is applied the dipolar particles tend to align along the field direction. The resulting transition from the inhomogeneous zero-field configuration to the homogeneously magnetized state in the presence of strong fields can also be examined within the present approach. We have applied the field normal to the surfaces of the cube but in different directions relative to the spontaneously chosen vortex axis of the zero-field configuration, which was used as an initial guess for the minimization algorithm. The most stable configurations turned out to be those for which the vortex axis is parallel to the external field. The relative stability of the resulting configurations can be judged

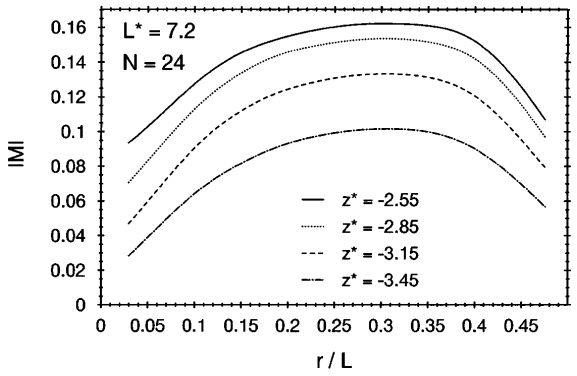

FIG. 2. Absolute value of the dimensionless magnetization as a function of the distance r from the vortex axis along lines parallel to the x or y axes at different heights $z^* = z/\sigma$. 24^3 mesh points are used and the side length is $L^* = L/\sigma = 7.2$. Around the point defect at the center of the bottom face the degree of orientational order is strongly reduced.

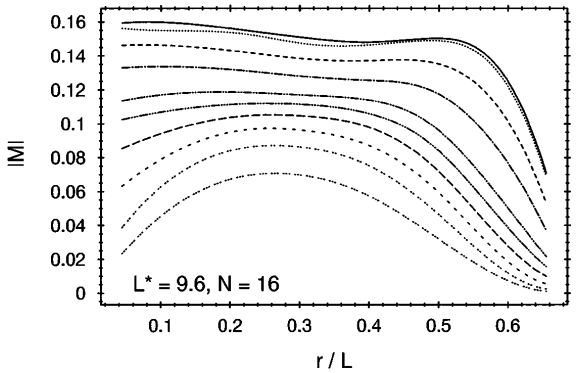

FIG. 3. Absolute value of the magnetization along diagonal lines near the midplane ($z \simeq 0$) as a function of the temperature. From top to bottom the lines correspond to the following values of T^*: 2.25; 2.30 to 2.60 in steps of 0.10; 2.65 to 2.85 in steps of 0.05. The estimated Curie temperature is $T_c^* = 2.89$. Near the vortex axis ($r = 0$) $|\mathbf{M}|$ decreases faster than for intermediate values of r so that a column of less ordered fluid develops around this axis.

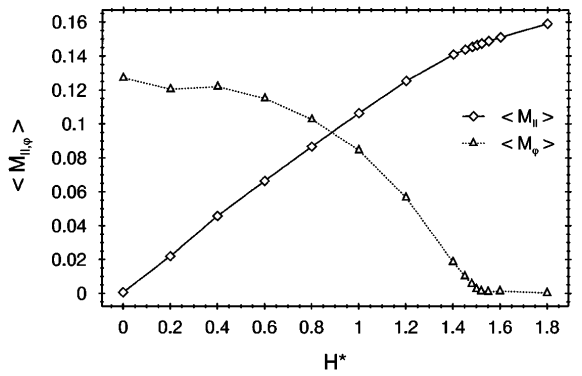

FIG. 4. Dependence of the averaged longitudinal magnetization component $\langle M_{\parallel}\rangle$ and the averaged angular component $\langle M_{\varphi}\rangle$ on the field strength for fixed temperature $T^* = 2.25$. The angular component decreases for increasing $H^* = H\sqrt{\sigma^3/\epsilon}$ and vanishes approximately linearly at $H_c^* \simeq 1.50$. Below H_c^* the parallel component increases approximately linearly and crosses over towards saturation for $H^* > H_c^*$. Above H_c^* the sample has an approximately uniform magnetization. The data correspond to $L/\sigma = 9.6$ and 16^3 mesh points.

on the basis of the corresponding value of the free energy. At moderate field strengths the in-plane structure perpendicular to the vortex axis is essentially preserved, while there is a substantial increase of the magnetization component parallel to the field. If the field is sufficiently strong the vortex structure is lost at a critical field strength H_c. This is shown in Fig. 4 by the field dependence of the averaged parallel component $\langle M_{\parallel}\rangle = N^{-3}\sum_{\mathbf{R}} M_3(\mathbf{R})$ and of the angular component $\langle M_{\varphi}\rangle = N^{-3}\sum_{\mathbf{R}} \mathbf{e}_{\varphi}(\mathbf{R}) \cdot \mathbf{M}(\mathbf{R})$, where $\mathbf{e}_{\varphi}(\mathbf{R}) = (R_2, -R_1, 0)/|\mathbf{R}|$.

In metallic liquid ferromagnets short-ranged exchange interactions due to the conduction electrons, which are not incorporated in the present theory, play a dominant role and determine the Curie temperature. However, once the system is ferromagnetically ordered the inevitable presence of additional long-ranged dipolar interactions leads to the formation of an inhomogeneous magnetization structure. Thus we expect the large scale domain structures of these systems to be similar to those of purely dipolar fluids, as described in this work. In liquids the spatial structure of the orientational order differs from the domain structure in ferromagnetic solids due to the absence of lattice anisotropies. An experimental study of this structure, e.g., using magnetic neutron tomography or x-ray microscopy based on x-ray magnetic circular dichroism [29] would certainly be very rewarding and important for determining the equilibrium shapes of ferromagnetic liquid drops.

S. D. acknowledges helpful discussions with D. Thouless. We are grateful to R. Evans for a critical reading of the manuscript.

[1] D. Wei and G. N. Patey, Phys. Rev. Lett. **68**, 2043 (1992).
[2] D. Wei and G. N. Patey, Phys. Rev. A **46**, 7783 (1992).
[3] J. J. Weis, D. Levesque, and G. J. Zarragoicoechea, Phys. Rev. Lett. **69**, 913 (1992).
[4] J. J. Weis and D. Levesque, Phys. Rev. E **48**, 3728 (1993).
[5] M. J. Stevens and G. S. Grest, Phys. Rev. E **51**, 5962 (1995).
[6] M. J. Stevens and G. S. Grest, Phys. Rev. E **51**, 5976 (1995).
[7] K. Sano and M. Doi, J. Phys. Soc. Jpn. **52**, 2810 (1983).
[8] H. Zhang and M. Widom, Phys. Rev. E **49**, R3591 (1994).
[9] D. Wei, G. N. Patey, and A. Perera, Phys. Rev. E **47**, 506 (1993).
[10] B. Groh and S. Dietrich, Phys. Rev. Lett. **72**, 2422 (1994); **74**, 2617 (1995).
[11] B. Groh and S. Dietrich, Phys. Rev. E **50**, 3814 (1994).
[12] D. Platzek, C. Notthoff, D. M. Herlach, G. Jacobs, D. Herlach, and K. Maier, Appl. Phys. Lett. **65**, 1723 (1994).
[13] J. Reske, D. M. Herlach, F. Keuser, K. Maier, and D. Platzek, Phys. Rev. Lett. **75**, 737 (1995).
[14] M. Widom and H. Zhang, Phys. Rev. Lett. **74**, 2616 (1995).
[15] B. Groh and S. Dietrich, Phys. Rev. E **53**, 2509 (1996).
[16] R. B. Griffiths, Phys. Rev. **176**, 655 (1968).
[17] J. J. Weis, M. J. P. Nijmeijer, J. M. Tavares, and M. M. Telo da Gama, Phys. Rev. E **55**, 436 (1997), and references therein.
[18] N. D. Mermin, Rev. Mod. Phys. **51**, 591 (1979).
[19] P. Frodl and S. Dietrich, Phys. Rev. A **45**, 7330 (1992); Phys. Rev. E **48**, 3203 (1993).
[20] W. H. Press, B. P. Flannery, S. A. Teukolsky, and W. T. Vetterling, *Numerical Recipes* (Cambridge University Press, Cambridge, 1989); simulated annealing is a stochastic numerical method to find the minimum of a complicated function of many variables and thus should be distinguished from a Monte Carlo simulation.
[21] H. B. Lavender, K. A. Iyer, and S. J. Singer, J. Chem. Phys. **101**, 7856 (1994).
[22] D. Lu and S. J. Singer, J. Chem. Phys. **103**, 1913 (1995).
[23] W. Williams and D. J. Dunlop, Nature (London) **337**, 634 (1989).
[24] A. J. Newell, D. J. Dunlop, and W. Williams, J. Geophys. Res. **98**, 9533 (1993).
[25] W. F. Brown Jr., *Micromagnetics* (Krieger, Huntington, 1978).
[26] A. Hubert, in *Theorie der Domänenwände in geordneten Medien*, edited by J. Ehlers, K. Hepp, and H. A. Weidenmüller, Lecture Notes in Physics (Springer, Berlin, 1974), Vol. 26.
[27] P. G. de Gennes and P. A. Pincus, Solid State Commun. **7**, 339 (1969).
[28] Strictly speaking the finite sample size leads to a rounding of the phase transition which, however, is not captured by the present mean field theory.
[29] G. Schmahl, P. Guttmann, D. Raasch, P. Fischer, and G. Schütz, Synchrotron Radiation News **9**, 35 (1996).